

# Spectroscopic Properties and Conformational Features of Short Linear Peptides in Solution: A Fluorescence and Molecular Mechanics Investigation

B. Pispisa,<sup>1,4</sup> C. Mazzuca,<sup>1</sup> A. Palleschi,<sup>1</sup> L. Stella,<sup>1</sup> M. Venanzi,<sup>1</sup> F. Formaggio,<sup>2</sup>  
C. Toniolo,<sup>2</sup> J. -P. Mazaleyrat,<sup>3</sup> and M. Wakselman<sup>3</sup>

Received July 19, 2002; revised October 7, 2002; accepted October 8, 2002

The ground- and excited-state properties of two conformationally constrained hexapeptides of general formula Boc-Bin-A<sub>1</sub>-A<sub>2</sub>-T-A<sub>1</sub>-A<sub>2</sub>-OtBu, where A<sub>1</sub> and A<sub>2</sub> are  $\alpha$ -aminoisobutyric acid (Aib) or L-alanine (Ala), Bin is an optically pure, axially chiral 1,1'-binaphthyl-substituted Aib, and T (Toac) is a stable nitroxide free radical-containing Ac6c analog, were investigated in methanol solution. These peptides are denoted as (*R*)-Bin/Toac and (*S*)-Bin/Toac, depending on the chirality of the binaphthyl moiety. Electronic spectra in methanol indicate the occurrence of intramolecular exciton interaction between the naphthyl moieties of Bin, and time-resolved fluorescence measurements show a biexponential decay for both peptides examined. According to infrared (IR) absorption data in the NH stretching frequency region, and to earlier X-ray diffraction results on (*S*)-Bin/Toac in the crystal state, both (*R*)-Bin/Toac and (*S*)-Bin/Toac populate a  $3_{10}$ -helix in solution with opposite screw sense, the helical handedness being determined by the chirality of binaphthyl and not by that of the Ala residues in the main chain. The combination of molecular mechanics calculations with fluorescence decay data indicate that the two observed lifetimes for each peptide arise from two conformations having different interprobe distance and orientation, in which electronic energy transfer from excited Bin to Toac takes place.

**KEY WORDS:** Steady-state fluorescence; time-resolved fluorescence;  $3_{10}$ -helical peptides; electronic energy transfer; Förster model; molecular mechanics calculations; molecular modeling.

## INTRODUCTION

Peptide helices of different length have been used as spacers in photophysical studies, in that rigid D-spacer-A assemblies (where D is a donor and A an acceptor group) provide a well-defined distance and orientation between the probes, thus facilitating a correct

interpretation of experimental results based on geometric-dependent photophysical processes [1,2]. This is particularly true for peptides exhibiting a restricted conformational mobility, comprising C <sup>$\alpha$</sup> -disubstituted  $\alpha$ -amino acids in the backbone chain [3,4].

With the aim of elucidating the dynamics and conformational features of linear, sterically restrained oligopeptides in solution [5] carrying appropriate fluorophores, we investigated the photophysical behavior of two short, linear peptides containing covalently linked (*R*)- or (*S*)-binaphthyl [(*R*)- or (*S*)-Bin] and Toac (T), as illustrated in Chart I. The general formula of these hexapeptides is Boc-Bin-A<sub>1</sub>-A<sub>2</sub>-T-A<sub>1</sub>-A<sub>2</sub>-OtBu, where A<sub>1</sub> and A<sub>2</sub> are  $\alpha$ -aminoisobutyric acid (Aib) or L-alanine (Ala), Boc is *tert*-butyloxycarbonyl, OtBu *tert*-butoxy, and Toac is

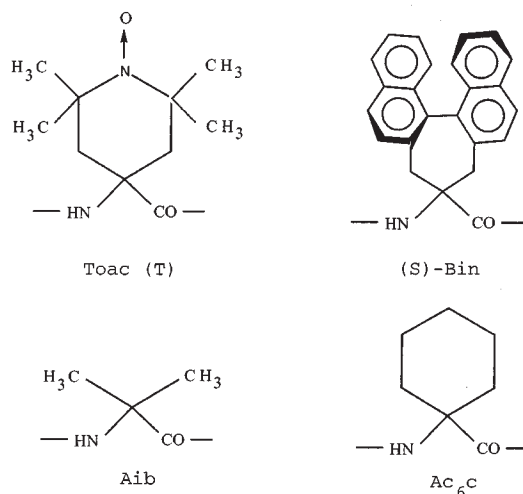
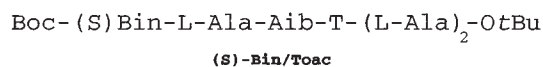
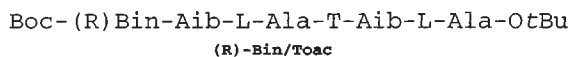
<sup>1</sup> Dipartimento di Scienze e Tecnologie Chimiche, Università di Roma Tor Vergata, 00133 Roma, Italy.

<sup>2</sup> Istituto di Chimica Biomolecolare, C.N.R., Dipartimento di Chimica Organica, Università di Padova, 35131 Padova, Italy.

<sup>3</sup> SIRCOB, Bât. Lavoisier, Université de Versailles, 7800 Versailles, France.

<sup>4</sup> To whom correspondence should be addressed. E-mail: pispisa@stc.uniroma2.it

CHART I



2,2,6,6-tetramethylpiperidine-1-oxyl-4-amino-4-carboxylic acid. One of the questions to address was the role played by the chirality of Bin, located at the N-terminus of the main chain, on the screw sense of the helical backbone. According to X-ray diffraction data in the crystal state [6,7], the (S)-Bin/Toac hexapeptide is in the  $3_{10}$ -helical conformation with left-handedness (l.h.), despite the presence of L-alanine residues in the backbone chain. In addition, because the X-ray analysis of this peptide shows the presence of two conformers, which have different puckering of the Toac moiety and its spatial orientation with respect to the Bin group [6,7], another question was whether a conformational equilibrium of this type takes place in solution. By combining time-resolved fluorescence measurements with molecular mechanics calculations, we were able to build up the sterically most favored conformations in solution, which for (S)-Bin/Toac were found to well reproduce the structural features of the crystal state. This finding emphasized the lack of conformational mobility in the peptides examined.

## EXPERIMENTAL

The syntheses of the Bin/Toac hexapeptides were performed step-by-step in solution. Bin [8] and Toac residues were incorporated using the *N*-ethyl, *N'*-(3-

dimethyl-aminopropyl) carbodiimide/1-hydroxy-7-aza-benzo-triazole approach [9], whereas Aib and Ala residues were incorporated *via* the symmetrical anhydride method. Both compounds were obtained in a chromatographically homogeneous state and were fully characterized [7,10].

Spectrograde solvents (Fluka) were used; the CDCl<sub>3</sub> for IR spectra was 99.8% D.

Infrared (IR) absorption spectra were recorded on a Perkin-Elmer 983 spectrophotometer, using CaF<sub>2</sub> cells. Circular dichroism (CD) measurements were performed using a Jasco J-600 instrument with appropriate quartz cells.

Steady-state fluorescence spectra were recorded on a SPEX Fluoromax spectrofluorimeter, operating in the SPC mode. Nanosecond decays were measured using a CD900 SPC lifetime apparatus from Edinburgh Instruments. The decay curves were fitted by a nonlinear least squares analysis to exponential functions through an iterative deconvolution method. All solutions were bubbled for 20 min with ultrapure argon before each measurement.

Other instruments were described in references [5,11].

## RESULTS AND DISCUSSION

### IR Spectra

Helical peptides are known to exhibit two characteristic absorption bands in the NH stretching region, one at approximately 3430 cm<sup>-1</sup>, associated to the stretching vibration of N-H groups not involved in H-bond interactions, and the other one at approximately 3330 cm<sup>-1</sup>, typical of H-bonded N-H groups. We measured the ratio of the integrated molar extinction coefficients  $\epsilon_b/\epsilon_f$  (where subscripts b and f denote H-bonded and free NH groups, respectively) for both (R)- and (S)-Bin/Toac hexapeptides. This ratio was obtained from the integrated IR absorbances of intramolecularly H-bonded (A<sub>b</sub>) and free (A<sub>f</sub>) N-H groups, according to the expression  $\epsilon_b/\epsilon_f = (A_b/A_f)(n_f/n_b)^{11}$ , where  $n_b$  and  $n_f$  are the numbers of H-bonded and free peptide units, respectively. From the results, one obtains  $\epsilon_b/\epsilon_f = 2.8 \pm 0.4$  and  $3.7 \pm 0.4$  for (R)- Bin/Toac and (S)-Bin/Toac, respectively [12]. Within experimental errors, these figures fall on the curve earlier determined for a number of  $3_{10}$ -helical peptides [11], thereby indicating that the Bin/Toac peptides examined populate a  $3_{10}$ -helix, which, in turn, implies that the ordered structure in the crystal state [6,7] is fully preserved in solution.

### Ground- and Excited-State Properties

The ultraviolet (UV) absorption spectra of (R)- and (S)-Bin/Toac in methanol and the UV spectrum of the

reference [(*S*)-Bin] exhibit a shift to 305 nm of the naphthalene band at 280 nm, whereas the band at approximately 225 nm is doubled. The maxima are found at 218 and 230 (sh) nm. This finding implies a strong electronic coupling of naphthyl moieties in the ground state via intramolecular exciton interaction [13,14]. The exciton is delocalized over the entire binaphthyl group, causing an exciton splitting in the circular dichroism spectrum (Fig. 1)[15].

The presence of Toac in the molecules does not perturb such strong coupling, according to the finding that both the absorption and CD spectra of the Bin/Toac peptides are almost identical to those of the reference. In addition, no charge transfer bands are detected in the electronic spectra, ruling out the formation of a ground-state CT complex.

We next examined the excited-state behavior of the Bin/Toac peptides. According to steady-state fluorescence spectra in methanol ( $\lambda_{\text{ex}} = 305$  nm), a substantial quenching of Bin singlet emission by Toac occurs (Fig. 2), although no evidence for exciplex emission could be obtained, even by decreasing solvent polarity (methanol vs dioxane).

For time-resolved fluorescence behavior ( $\lambda_{\text{ex}} = 305$  nm,  $\lambda_{\text{em}} = 360$  nm), the decay curve of the reference was found to be strictly monoexponential, i.e.,  $\tau_0 = 4.9$  ns in methanol, with  $\tau_0$  definitely shorter than the unperturbed lifetime of naphthalene (52.5 ns). This indicates a strong dynamic quenching, very likely ascribable to an exciton interaction associated with the aforementioned coupling regime. In contrast, the Bin/Toac hexa-

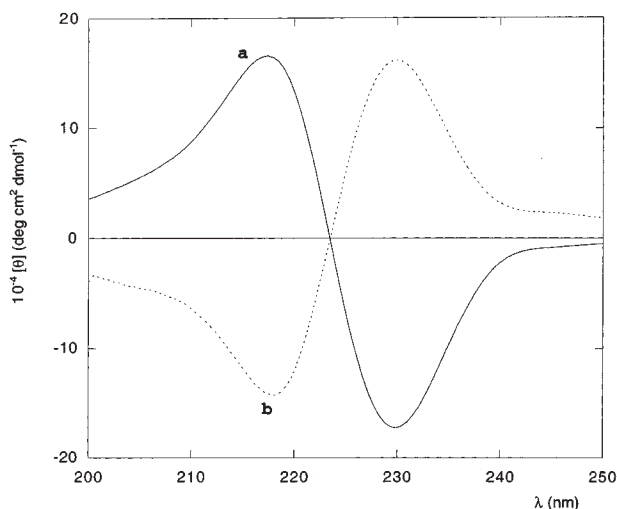


**Fig. 1.** CD spectra of (*R*)-Bin/Toac (a) and (*S*)-Bin/Toac (b) in methanol, within the wavelength region of binaphthyl absorption.

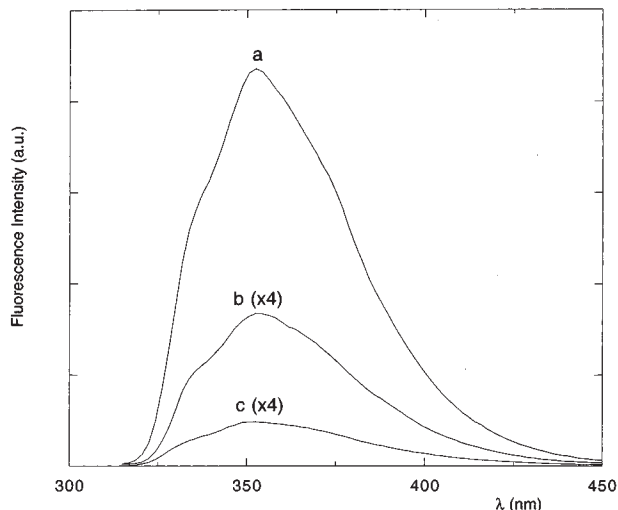


**Fig. 2.** Steady-state fluorescence spectra of the reference (*S*)-Bin (a), (*S*)-Bin/Toac (b), and (*R*)-Bin/Toac (c) in methanol, at approximately  $2 \times 10^{-6}$  M concentration.

peptides exhibit a biexponential decay, according to the expression

$$I(t) = \sum_i \alpha_i \exp(-t/\tau_i) \quad (1)$$

where  $i = 1$  or 2 (Fig. 3).

The lifetime distribution analysis of the decays is in full agreement with the results of the discrete model reported in Table I. The results give one distribution only for the reference and two narrow distributions for

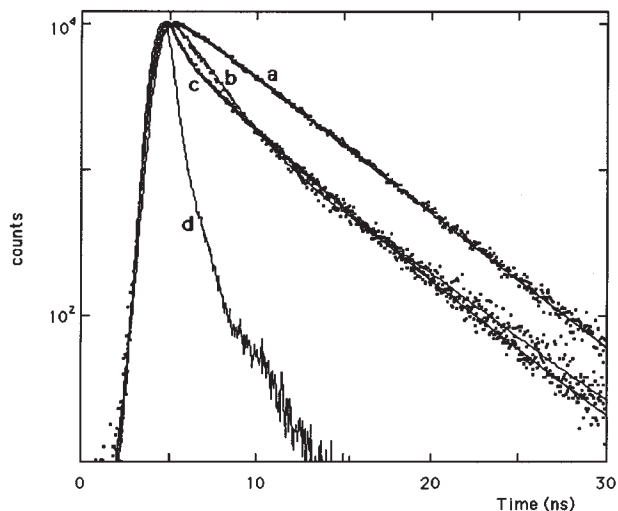


**Fig. 3.** Normalized decay profile ( $\lambda_{\text{ex}} = 305$ ,  $\lambda_{\text{em}} = 360$  nm) for the reference (a), (*S*)-Bin/Toac (b), and (*R*)-Bin/Toac (c) in methanol. The full lines represent the best fit to the experimental data by a mono- (a) and a biexponential (b and c) decay. The lamp profile is also shown (d).

**Table I.** Time Decay Parameters of Excited Bin in the (*S*)- and (*R*)-Bin/Toac Hexapeptides in Methanol,<sup>a</sup> from Both Exponential (ex) and Lifetimes Distribution (ld) Analyses

Peptide	Data analysis	$\alpha_1$	$\tau_1$ (ns)	Distribution width <sup>b</sup> (ns)	$\alpha_2$	$\tau_2$ (ns)	Distribution width <sup>b</sup> (ns)	$\chi^2$
( <i>S</i> )-Bin/Toac	ex	0.79	1.36		0.21	4.46		1.33
	ld	0.82	1.54	0.63	0.18	4.70	0.74	1.33
( <i>R</i> ) - Bin/Toac	ex	0.74	0.47		0.26	4.36		1.13
	ld	0.69	0.43	0.22	0.31	4.16	0.80	1.17

<sup>a</sup>  $\lambda_{\text{ex}} = 305$ ,  $\lambda_{\text{em}} = 360$  nm. The uncertainty in the lifetimes is approximately 10%, but it is within  $\pm 0.15$  ns for the shortest lifetime from the exponential analysis. The uncertainty in the preexponents is approximately 10%.

<sup>b</sup> Full width at half-maximum.

both (*S*)- and (*R*)-Bin/Toac hexapeptides, the centers and relative weights of which compare well with the lifetimes and preexponents of the discrete model, respectively (Table I). This finding strongly supports the idea that each decay component of the discrete model refers to one conformer populating the solution, characterized by a given center-to-center distance and mutual orientation of the chromophores. In principle, a single decay time could arise either from a single conformer or from many conformers, all having a very similar quenching rate. This latter hypothesis implies that all of these conformers have a very similar structure, and hence a very similar interprobe distance and orientation; they are thus indistinguishable within the resolution time. Interestingly, the distribution analysis of the fluorescence time decay of (*S*)-Bin/Toac in dimethylsulfoxide (DMSO, a well-known structure-breaking solvent) gives rise to one wide distribution only, very likely arising from many slightly different conformations. This is a further indication that each lifetime of the biexponential decay in methanol, listed in Table I, is ascribable to one conformer only.

Finally, the observation that  $\langle\tau\rangle/\tau_0 \neq \Phi/\Phi_0$ , where  $\langle\tau\rangle = \sum_i \alpha_i \tau_i$  and indicates that static quenching occurs in both peptides,  $\langle\tau\rangle/\tau_0$  is  $0.41 \pm 0.06$  and  $0.30 \pm 0.06$ , as compared with  $\Phi/\Phi_0 = 0.10 \pm 0.02$  and  $0.03 \pm 0.01$  for the (*S*)- and (*R*)-Bin/Toac, respectively. This effect is likely to arise from an instantaneous process within a complex between the active chromophores. In addition, the observation that the ratio of the average lifetimes of (*S*)-Bin/Toac and (*R*)-Bin/Toac is quite different from the ratio of the corresponding quantum yields of the steady-state spectra (i.e., 1.36 compared with 3.50), suggests that the aforementioned ground-state complexes populate the solution to a different extent. This finding is not surprising because the two peptides are diastereomers; they have different structural features and experience different short-range interactions. A difference in the energetics should be expected.

## Quenching Mechanism

We then addressed the problem of the mechanisms that contribute to the singlet state quenching in the Bin/Toac hexapeptides. Despite the widespread use of doublet quenchers to probe the structural and dynamic features of membranes [16,17], micelles [18], and protein surfaces [19,20], there is no univocal interpretation of this phenomenon yet, chiefly because most of the literature about nitroxide-based quenchers describe uncovalently linked fluorophore-quencher pairs, leading to measured quenching rate constants controlled by diffusion processes [19].

We first investigated the electron transfer (ET) within the hexapeptides. This quenching pathway, however, was ruled out because of the lack of correlation between the polarity of the solvents used and the kinetics of the intramolecular ET process. One would have expected large dynamic solvent effects on the rate constants [21]. In contrast, the quenching rate constants were as follows:  $k_1 = 5.3 \times 10^8 \text{ s}^{-1}$  and  $k_2 = 2.0 \times 10^7 \text{ s}^{-1}$  in methanol ( $\epsilon = 32.7$ );  $k_1 = 16.4 \times 10^8 \text{ s}^{-1}$  and  $k_2 = 6.5 \times 10^7 \text{ s}^{-1}$  in isopropyl alcohol ( $\epsilon = 18.9$ );  $k_1 = 9.1 \times 10^8 \text{ s}^{-1}$  and  $k_2 = 5.1 \times 10^7 \text{ s}^{-1}$  in dioxane ( $\epsilon = 2.0$ ), where  $k_i = \tau_i^{-1} - \tau_0^{-1}$ .

We next examined the quenching mechanism in terms of Dexter [22] and Förster [23] models.

The efficiency in the Dexter energy transfer mechanism is exponentially dependent on the interchromophoric distance [24]:

$$E_i/(1-E_i) = (2\pi/k_D)V_i J_D \quad (2)$$

where  $i = 1$  or  $2$ ,  $k_D = \tau_0^{-1}$  is the rate constant for the donor emission, and  $J_D$  is the Dexter overlap integral (cm), as obtained by spectroscopic measurements, i.e.:

$$J_D = \int_0^\infty F_{i,D}(\bar{\nu}) \epsilon_{i,A}(\bar{\nu}) d\bar{\nu} \quad (3)$$

with the normalization conditions:

$$\int_0^{\infty} F_{i,D}(\bar{\nu})d\bar{\nu} = \int_0^{\infty} \epsilon_A(\bar{\nu})d\bar{\nu} = 1 \quad (4)$$

whereas

$$V_{m^2} = K_m \exp(-2R_m/L) \quad (5)$$

In Eq. (5),  $K_m$  is a constant corresponding to the electronic matrix coupling at orbital contact,  $R_m$  is the inter-probe center-to-center distance in the  $m$ th conformer of the given peptide, and  $L$  is the average radius involved in the initial and final states [25]. By using the same  $L = 5.0 \text{ \AA}$  value for the van der Waals radius of the probes in both peptides examined, the  $K_m \cdot J_D$  values are approximately  $4 \times 10^{-18} \text{ erg}$ , i.e., one order of magnitude higher than those reported for electronic energy transfer via exchange interaction in bichromophoric molecules [26]. This strongly suggests that the intramolecular energy transfer in both (*R*)- and (*S*)-Bin/Toac hexapeptides is not controlled by a Dexter-type mechanism.

We have studied the photophysics of a number of assemblies carrying Toac as acceptor and tryptophan [5] and fluorene [27] as donor. In all cases, the quenching mechanism could be correctly described by the Förster model [23,28], for which rate constant for energy transfer can be expressed as:

$$k_{m,F} = 8.71 \times 10^{23} \times (J_F \kappa_m^2 \Phi_0) / (R_m^6 n^4 \tau_0) \quad (6)$$

where  $J_F$  is the overlap integral calculated from fluorescence spectra, as given by Eq. (7),  $\kappa_m^2$  is a dimensionless geometric parameter determined by the spatial orientation of the transition dipole moments of the donor and acceptor in the  $m$ th conformer [5,29],  $\Phi_0$  is the quantum yield of the reference, and  $n$  is the refractive index of the solvent. Where rapid relative rotations occur, the dynamic isotropic average of the orientation factor,  $\langle \kappa^2 \rangle = 2/3$ , is instead used [29].

$$J_F = \frac{\int_0^{\infty} F_D(\bar{\nu}) \epsilon_A(\bar{\nu}) \bar{\nu}^{-4} d\bar{\nu}}{\int_0^{\infty} F_D(\bar{\nu}) d\bar{\nu}} \quad (7)$$

In Eq. (7),  $F_D(\bar{\nu})$  is the fluorescence intensity of the donor (Bin), and  $\epsilon_A(\bar{\nu})$  is the extinction coefficient of the acceptor (Toac) at wavenumber  $\bar{\nu}$ . Accordingly, the quenching efficiency can be written as [23,24,30]:

$$E_m = \frac{1}{1 + \left[ \frac{2}{3\kappa_m^2} \left( \frac{R_m}{R_0} \right)^6 \right]} \quad (8)$$

where  $R_0$  is the distance at which 50% transfer of excitation energy occurs, i.e.,

$$R_0 = 9.79 \times 10^3 [(2/3\Phi_0 J_F)/n^4]^{1/6} \quad (9)$$

Note that the transition dipole moment of Toac was taken to lie in the CNC plane [31] and perpendicular to the N–O bond, whereas that of the binaphthyl was taken as a vectorial combination of the dipoles from each naphthalene group, as shown in Fig. 4.

From the results,  $R_0 = 9.7 \text{ \AA}$  in methanol. Despite the relatively low  $R_0$  value, the Förster model is adequate to describe the quenching process in the peptides examined, as strongly suggested by the excellent agreement between the experimental and calculated quenching efficiencies, shown below. Furthermore, deviations from Förster theory at short distances have been extensively studied by Scholes and Ghiggino [32], who demonstrated that at separation of  $9 \text{ \AA}$  or more, the rate takes on the form expected for a pure dipole–dipole mechanism, whereas the exchange mechanism makes only a 5% contribution at  $5 \text{ \AA}$  separation. Several other articles support this conclusion [1,7], and recently, the Dexter mechanism was reported to apply only to compounds exhibiting  $R_0 \leq 5 \text{ \AA}$  [25].

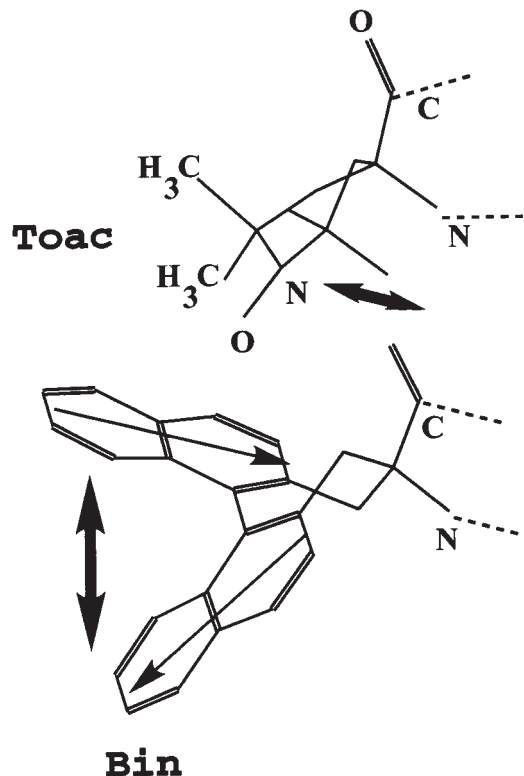


**Fig. 4.** Scheme of the two chromophores in the Bin/Toac peptides and of their electric dipole transition moments, represented as heavy double arrows.



To summarize, both theoretical and experimental results strongly support the idea that the dipole–dipole interaction is the major pathway of quenching in the peptides examined.

### Molecular Mechanics Calculations

To gather information on the geometric and steric constraints that control both the interchromophoric distance and probe orientation in the hexapeptides investigated, we have undertaken molecular mechanics calculations [33–35], starting from the backbone chain in both a l.h. and a right-handed (r.h.)  $3_{10}$ -helix, in agreement with the aforementioned IR data. The force field employed has been described [33,35] by  $U_{m,\text{tot}}$ , which denotes the total potential energy of the  $m$ th conformer [Eq. (11)], comprising stretching and bending terms (STR and BEN), in addition to electrostatic (COUL), nonbonding (NB), and torsional (TOR) potentials.

$$U_{m,\text{tot}} = \text{COUL} + \text{NB} + \text{TOR} + \text{STR} + \text{BEN} \quad (11)$$

Owing to the rigidity of the hexapeptides examined, a narrow distribution of conformers for each backbone structure could be predicted. As Table II lists the molecular parameters of the low-energy structures of the Bin/Toac peptides. The molecular models are illustrated in Fig. 5.

The main inferences to be drawn from Table II and Fig. 5 are as follows. First, the sterically most favored structures are two conformers with the backbone chain

with opposite screw sense, i.e., two r.h.  $3_{10}$ -helical conformers for (*R*)-Bin/Toac and two (isoenergetic) l.h.  $3_{10}$ -helical structures for (*S*)-Bin/Toac. Second, in both cases these conformers experience a different spatial orientation of Toac with respect to (*R*)- or (*S*)-Bin, owing to a different puckering of the Toac moiety. Third, the topology of the Toac ring in the computed conformations is close to that observed in the crystal state for (*S*)-Bin/Toac, as illustrated in Table III.

Finally, in both cases molecular mechanics calculations give rise to an additional conformer with a low population, which might be associated with the non-fluorescent ground-state complex mentioned above. This will be discussed elsewhere, though it is worth noting that molecular mechanics underestimate the population of these complexes because electronic effects could not be taken into account.

### Comparison Between Experimental and Theoretical Results

When the experimental quenching efficiency, as given by

$$E_i = 1 - (\tau_i / \tau_0) \quad (10)$$

is compared with that theoretically obtained from the computed low-energy structures, according to Eq. (8), a very good agreement is obtained, as shown in Table II. This validates the computed structures in that the correlation between calculated and experimental efficiencies

**Table II.** Molecular Parameters and Energy Transfer Efficiencies in the Sterically Most-Favored Conformers of (*S*)- and (*R*)-Bin/Toac Hexapeptides

Backbone conformation <sup>a</sup>	$U_{m,\text{tot}}$ <sup>b</sup>	$R_m$ <sup>c</sup>	$\kappa_m$ <sup>2d</sup>	$E_{m,\text{calcd}}$ <sup>e</sup>	$E_{i,\text{exp}}$ <sup>f</sup>
<b>(<i>S</i>)-Bin/Toac</b>					
l.h. $3_{10}$ -helix <sup>g</sup>	0	5.84	0.090	0.74	0.72, 0.07
	0	6.18	0.004	0.07	
r.h. $3_{10}$ -helix	1.7	8.69	0.700	0.67	
<b>(<i>R</i>)-Bin/Toac</b>					
r.h. $3_{10}$ -helix <sup>g</sup>	0	7.23	0.765	0.87	0.90, 0.09
	0.31	7.26	0.021	0.15	
l.h. $3_{10}$ -helix	3.1	9.60	0.417	0.40	

<sup>a</sup> Left-handed (l.h.) and right-handed (r.h.) helix.

<sup>b</sup> From Eq. (11) (kcal · mol<sup>-1</sup>).

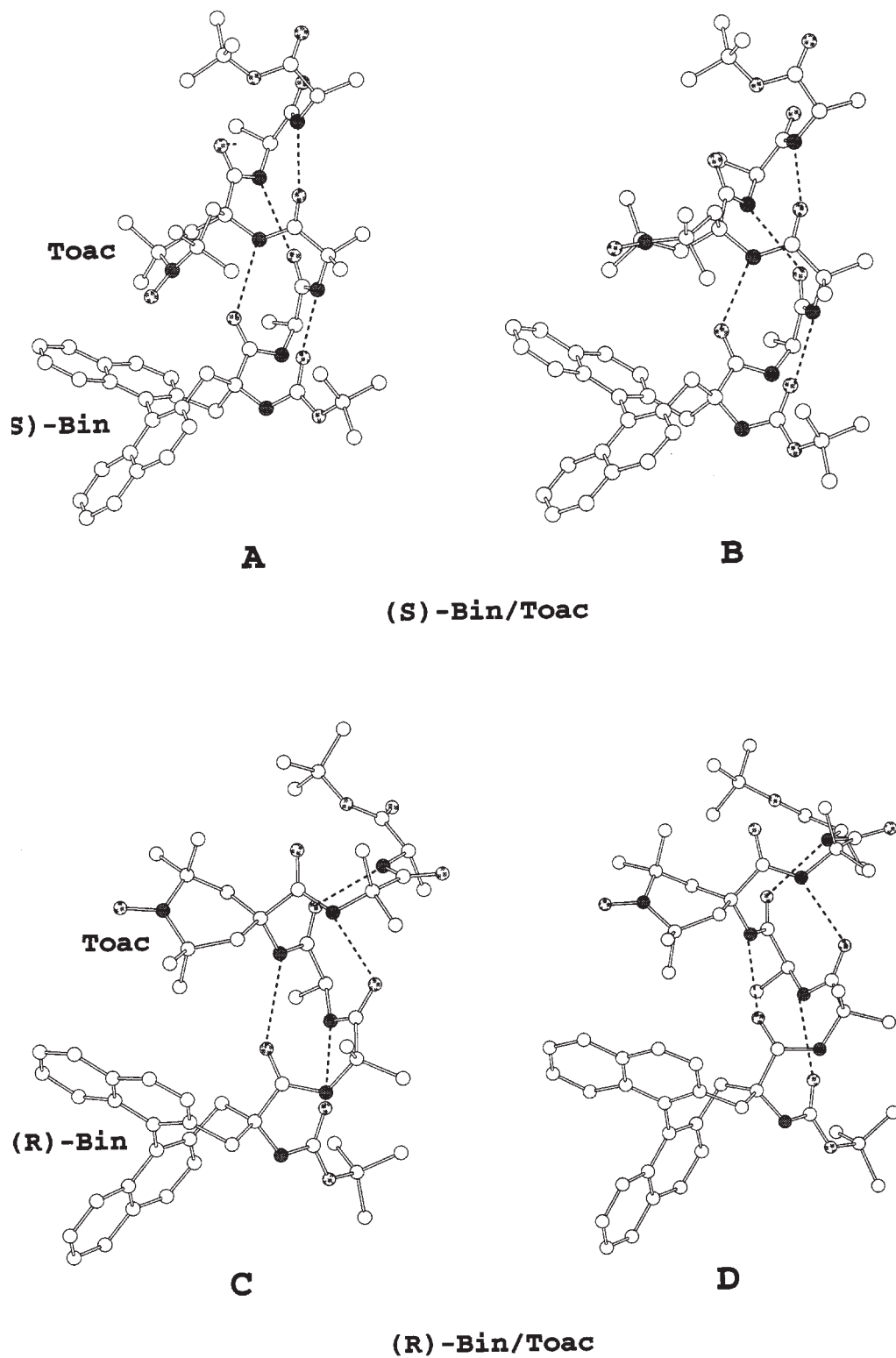
<sup>c</sup> Interchromophoric center-to-center distance (Å).

<sup>d</sup> Orientation parameter.

<sup>e</sup> Calculated energy transfer efficiency, from Eq. (8).

<sup>f</sup> Experimental energy transfer efficiency (in methanol), as given by Eq 10.

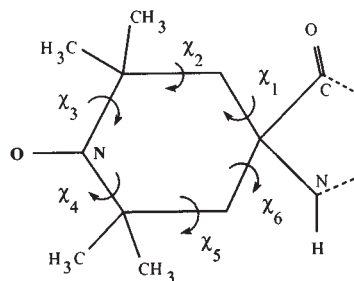
<sup>g</sup> See Fig. 5.



**Fig. 5.** Molecular models of the sterically most favored conformers of (S)-Bin/Toac (A and B) and (R)-Bin/Toac (C and D). The backbone chain is in the left-handed (l.h.) and right-handed (r.h.)  $3_{10}$ -helix, respectively, viewed perpendicularly to the helical axis. In each structure, the four intramolecular H-bonds are indicated by dashed lines. Nitrogen atoms are in black and oxygen atoms are dotted. Note the peculiarity of the handedness of the ordered backbone, which is not controlled by the chirality of the Ala residues, but rather by the chirality of the binaphthyl moiety at the N-terminus of the main chain. Note also the close approach of one methyl group of Toac to one naphthyl moiety of Bin in all conformers, causing the chromophores to experience C-H ...  $\pi$  interactions that stiffen the whole molecule.

**Table III.** Comparison Between the Side-Chain Torsion Angles of Toac<sup>a</sup> in the Two Conformers of (*S*)-Bin/Toac Hexapeptide in the Crystal State<sup>b</sup> and in Methanol<sup>c</sup>

Conformers	$\chi_1$	$\chi_2$	$\chi_3$	$\chi_4$	$\chi_5$	$\chi_6$
X-ray structure (A)	3.9	-43.0	41.7	1.7	-46.7	43.4
X-ray structure (B)	20.4	-48.0	24.0	24.7	-55.2	33.2
Calculated structure in methanol (A)	-15.0	-33.0	48.3	-12.0	-40.4	53.4
Calculated structure in methanol (B)	24.5	-51.3	22.0	28.9	-57.3	30.2

<sup>a</sup><sup>b</sup> As determined by X-ray diffraction analysis [6,7].<sup>c</sup> In the deepest energy minimum, from molecular mechanics calculations.

is highly demanding for the structural features, and depends on the sixth power of the interprobe distance and the mutual orientation of the probes, and also on the spectroscopic parameter  $R_0$ , and hence on the properties of both the fluorophores and solvent [Eq. (8)]. Therefore, the low-energy computed conformers may be considered as a good representation of those actually populating the methanol solution.

## CONCLUSIONS

The Bin/Toac hexapeptides investigated experience electronic energy transfer from excited binaphthyl to ground-state Toac as the major excited-state process in the nanosecond time scale. Combination of time-resolved fluorescence resonance energy transfer measurements with molecular mechanics data were productive in solving the problem of a quick identification of the most relevant structural features of relatively small compounds in solution. This is an important goal for fluorescence spectroscopy, because even nuclear magnetic resonance (NMR) studies do not always lead to a unique interpretation of the conformational features of peptides in solution. Indeed, this kind of study is often made difficult by the large conformational changes occurring rapidly on the NMR time scale, so that the NMR observables and the restraints developed from them are only consistent with an average structure that may not even exist [36].

## ACKNOWLEDGMENTS

This work was supported by both the National Research Council (CNR) and MURST.

## REFERENCES

1. S. Speiser (1996) *Chem. Rev.* **96**, 1953–1976.
2. C. Dos Remedios and P. D. J. Moens (1999) in D. L. Andrews and A. A. Demidov (Eds.), *Resonance Energy Transfer*, Wiley, New York, Chapter 1.
3. C. Toniolo and E. Benedetti (1991) *Macromolecules* **24**, 4004–4009.
4. I. L. Karle and P. Balaram (1990) *Biochemistry* **29**, 6747–6756.
5. B. Pispisa, A. Palleschi, L. Stella, M. Venanzi, and C. Toniolo (1998) *J. Phys. Chem. B* **102**, 7890–7898.
6. C. Toniolo, F. Formaggio, M. Crisma, J.-P. Mazaleyrat, M. Wakselman, C. George, J. L. Flippen-Andersen, B. Pispisa, M. Venanzi, and A. Palleschi (1999) in J. P. Tam and P. T. P. Kaumaya (Eds.), *Peptides: Frontiers of Peptide Science*, Kluwer, Dordrecht, pp. 378–380.
7. C. Toniolo, F. Formaggio, M. Crisma, J.-P. Mazaleyrat, M. Wakselman, C. George, J. R. Deschamps, J. L. Flippen-Anderson, B. Pispisa, M. Venanzi, and A. Palleschi (1999) *Chem. Eur. J.* **5**, 2254–2264.
8. J.-P. Mazaleyrat, A. Gaucher, J. Savrda, and M. Wakselman (1997) *Tetrahedron: Asymmetry* **8**, 619–631.
9. L. A. Carpino (1993) *J. Am. Chem. Soc.* **115**, 4397–4398.
10. M. Rainaldi, F. Formaggio, and C. Toniolo (2002), in preparation.
11. B. Pispisa, A. Palleschi, L. Stella, M. Venanzi, C. Mazzuca, F. Formaggio, C. Toniolo, and Q. B. Broxterman (2002) *J. Phys. Chem. B* **106**, 5733–5738, and references therein.
12. C. Corvaja, E. Sartori, A. Toffoletti, F. Formaggio, M. Crisma, C. Toniolo, J.-P. Mazaleyrat, and M. Wakselman (2002) *Chem. Eur. J.* **6**, 2775–2782.



13. T. Förster (1959) *Discuss. Faraday Soc.* **27**, 7–17.
14. G. D. Scholes, K. P. Ghiggino, A. M. Oliver, and M. N. Paddon-Row (1993) *J. Am. Chem. Soc.* **115**, 4345–4349.
15. F. Formaggio, C. Peggion, M. Crisma, C. Toniolo, L. Tchertanov, J. Guilhem, J.-P. Mazaleyrat, Y. Goubard, and M. Wakselman (2001) *Helv. Chim. Acta* **84**, 481–501.
16. J. Matko, K. Ohki, and M. Edidin (1992) *Biochemistry* **31**, 703–711.
17. J. Matko, A. Jenei, T. Wei, and M. Edidin (1995) *Cytometry* **19**, 191–200.
18. J. Karpiuk and R. Grabowski (1989) *Chem. Phys. Lett.* **160**, 451–456.
19. E. Asuncion-Punzalan and E. London (1995) *Biochemistry* **34**, 11460–11466.
20. M. Castanho and M. Prieto (1995) *Biophys. J.* **69**, 155–168.
21. In Solvation (1988) *Faraday Discuss. Chem. Soc.* **85**, 341–364.
22. D. L. Dexter (1953) *J. Chem. Phys.* **21**, 836–850.
23. T. Förster (1948) *Ann. Phys. (Leipzig)* **2**, 55–75.
24. A. Grinvald, E. Haas, and I. Z. Steinberg (1972) *Proc. Natl. Acad. Sci. U.S.A.* **69**, 2273–2277.
25. S.-T. Levy, M. B. Rubin, and S. Speiser (1992) *J. Am. Chem. Soc.* **114**, 10747–10756.
26. S. Speiser and J. Katriel (1983) *Chem. Phys. Lett.* **102**, 88–94.
27. B. Pispisa, C. Mazzuca, A. Palleschi, L. Stella, M. Venanzi, F. Formaggio, A. Polese, and C. Toniolo (2000) *Biopolymers* **55**, 425–435.
28. B. Pispisa, A. Palleschi, C. Mazzuca, L. Stella, A. Valeri, M. Venanzi, F. Formaggio, C. Toniolo, and Q. B. Broxterman (2002) *J. Fluoresc.*, in press.
29. B. W. van der Meer (1999) in D. L. Andrews and A. A. Demidov (Eds), *Resonance Energy Transfer*, Wiley, New York, Chapter 4.
30. J. R. Lakowicz (1999) *Principles of Fluorescence Spectroscopy* 2nd edn., Kluwer, New York, Chapter 3.
31. S. A. Green, D. J. Simpson, G. Zhou, P. S. Ho, and N. V. Blough (1990) *J. Am. Chem. Soc.* **112**, 7337–7342.
32. G. D. Scholes and K. P. Ghiggino (1994) *J. Phys. Chem. B* **98**, 4580–4590.
33. E. Chiessi, M. Branca, A. Palleschi, and B. Pispisa (1995) *Inorg. Chem.* **34**, 2600–2609.
34. B. Pispisa, L. Stella, M. Venanzi, and A. Palleschi (1999) *J. Peptide Res.* **54**, 353–360.
35. B. Pispisa, L. Stella, M. Venanzi, A. Palleschi, C. Viappiani, A. Polese, F. Formaggio, and C. Toniolo (2000) *Macromolecules* **33**, 906–915.
36. D. F. Mierke, M. Kurz, M. and H. Kessler (1994) *J. Am. Chem. Soc.* **116**, 1042–1049.